Accepted Manuscript

$C_{60}@C_3N_4$ nanocomposites as quencher for signal-off photoelectrochemical aptasensor with Au nanoparticle decorated perylene tetracarboxylic acid as platform

Liu Yang, Xia Zhong, Liaojing Huang, Hanmei Deng, Ruo Yuan, Yali Yua

PII: S0003-2670(19)30671-3

DOI: https://doi.org/10.1016/j.aca.2019.05.058

Reference: ACA 236822

To appear in: *Analytica Chimica Acta*

Received Date: 24 March 2019

Revised Date: 22 May 2019

Accepted Date: 24 May 2019

Please cite this article as: L. Yang, X. Zhong, L. Huang, H. Deng, R. Yuan, Y. Yua, $C_{60}@C_3N_4$ nanocomposites as quencher for signal-off photoelectrochemical aptasensor with Au nanoparticle decorated perylene tetracarboxylic acid as platform, *Analytica Chimica Acta*, https://doi.org/10.1016/j.aca.2019.05.058.

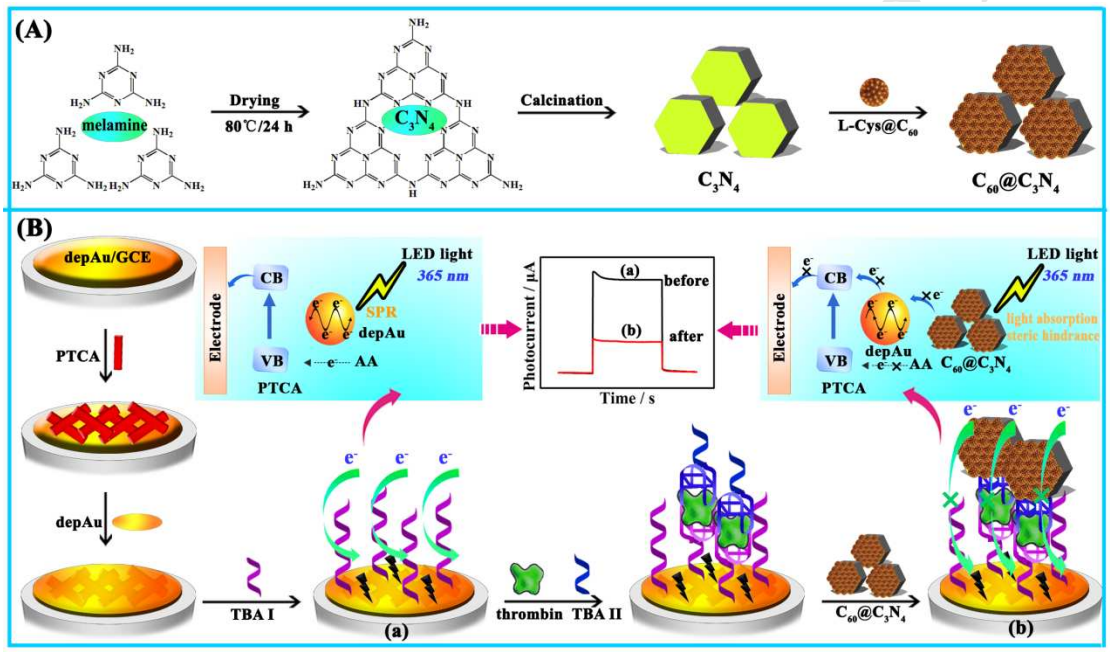

Graphic Abstract

$C_{60}@C_3N_4$ nanocomposites as quencher for signal-off photoelectrochemical aptasensor with Au nanoparticle decorated perylene tetracarboxylic acid as platform

Liu Yang, Xia Zhong, Liaojing Huang, Hanmei Deng, Ruo Yuan and Yali Yuan[a*]

Key Laboratory of Luminescent and Real-Time Analytical Chemistry (Southwest University), Ministry of Education, College of Chemistry and Chemical Engineering, Southwest University, Chongqing 400715, China

Abstract

Herein, a novel signal-off photoelectrochemical (PEC) aptasensor was proposed for sensitive detection of thrombin on the basis of $C_{60}@C_3N_4$ nanocomposites as quencher and Au nanoparticles (depAu) decorated perylene tetracarboxylic acid (PTCA) as sensing platform. Owing to the excellent membrane-forming of PTCA and superior conductivity of depAu, the PTCA between two depAu layers can simply and effectively produce an extremely high initial photocurrent to afford a precondition for sensitive biodetection. Thereafter, the assembly of $C_{60}@C_3N_4$ nanocomposites on electrode via typical sandwich reaction enabled the generation of a significantly decreased photocurrent. Here, the C_3N_4 with high surface area not only provided massive binding sites for C_{60} immobilization, but also partly competed with PTCA in light absorption for producing a significantly smaller photocurrent in the presence of electron donor ascorbic acid (AA). Additionally, both the C_3N_4 and C_{60} have the poor conductivity, which could inhibit the electron transfer to achieve a further decreased

photocurrent, effectively improving the sensitivity of proposed biosensor. As a result, the PEC biosensor in a "signal-off" mode showed an extremely low detection limit down to 1.5 fM, providing a sensitive and universal strategy for protein detection.

***Keywords*:** photoelectrochemical aptasensor; signal-off; light absorption; C_{60}@C_3N_4 nanocomposites; PTCA

1. Introduction

Thrombin is a highly specific serine endoprotease existed in the blood, which plays an important role in pathologic processes such as arterial thrombosis, leukemia and liver disease[1-3]. Accordingly, the quantitative and sensitive detection of thrombin is extremely important in fundamental research as well as clinical practice. Up to now, various intriguing bioanalytical methods, such as electrochemistry (EC)[1,4], photoelectrochemisty (PEC)[5-7], electrochemiluminescence (ECL)[8-10] fluorimetry (FL)[11,12], and chemiluminescence (CL)[13], have been developed for its detection. Among them, PEC-based detection system has received particular attention due to the separable excitation source (light) and detection signal (current) with significantly reduced background and improved sensitivity[14,15].

3,4,9,10-perylene tetracarboxylic acid (PTCA) is a conjugated organic dye with excellent membrane-forming. Its LUMO (π*) and HOMO (π) levels are -3.8 eV and -6.0 eV[16-18], respectively, providing a preeminent photoactive material with simple modification for PEC sensing system. Studies[19,20] have showed that the plasmonic Au nanoparticles as a photosensitizer for PTCA enabled the significant improvement of

photocurrent via surface plasmon resonance (SPR) process as well as light absorption. The electrons from the plasmonic nanoparticles can transfer immediately to the LUMO orbit of PTCA, followed by the migration to electrode with effective hindrance of the recombination for electron/hole pairs. Additionally, as we known, the electron donor/accepter can improve the photovoltaic conversion efficiency of some photoactive material through the oxidation-reduction reaction of donor/accepter. In our previous work, the ascorbic acid (AA) has proved to be a desirable electron donor for PTCA[5], thus providing a simple strategy with extremely high initial photocurrent to construct "signal-off" and signal tag "label-free" biosensor for sensitive biodetection.

Graphitic carbon nitride (C_3N_4) as a new polymer semiconductor has the superior advantages of simple preparation, high surface area and desirable band structure[21-23], thereby displays a predominant photovoltaic conversion efficiency in the assitant of electron donor, such as H_2O_2[24] and L-Cysteine[25]. Here, we found that the electron donor AA could also improve the photovoltaic conversion efficiency of C_3N_4, which however was much less than that of PTCA. Based on the observation, in this work, instead of being served as photoexcited material for signal output, the C_3N_4 was used as the carrier for loading inert fullerene (C_{60}) to form C_{60}@C_3N_4 nanocomposites, aiming to construct a C_{60}@C_3N_4 nanocomposites induced signal-off PEC aptasensor with Au nanoparticles (from electrodeposition, denoted as depAu) decorated PTCA as sensing platform. Owing to the excellent membrane-forming of PTCA[26] and SPR effect of depAu, the PTCA between two depAu layers was first performed on

electrode, which could simply and effectively produce an extremely high initial photocurrent to afford a precondition for sensitive biodetection in the assitant of electron donor AA. Interestingly, the C_3N_4 with high surface area not only provided massive binding sites for C_{60} immobilization, but also partly competed with PTCA in light absorption for producing a significantly smaller photocurrent in the presence of electron donor ascorbic acid (AA). After the immobilization of $C_{60}@C_3N_4$ nanocomposites on electrode via typical sandwich reaction, a significantly increased "signal-off" state could be acquired. Additionally, both the C_3N_4 and C_{60} have the poor conductivity, which could inhibit the electron transfer to achieve a further decreased photocurrent, effectively improving the sensitivity of PEC biosensor. By using $C_{60}@C_3N_4$ nanocomposites induced "signal-off" mode, a signal tag "label-free" PEC biosensor based on depAu/PTCA/depAu as sensing platform for ultrasensitive thrombin assay was readily realized.

2. Experimental sections

2.1 Preparation of $C_{60}@C_3N_4$ nanocomposites

Herein, the $C_{60}@C_3N_4$ nanocomposites were first prepared as follows: 1 mg C_{60} and 0.4 g L-Cys were simultaneously added into 1 mL PBS (pH 7.4) and subjected to an ultrasound for serval days until obtaining a dark brown solution. Then, the centrifugation was used to remove excess L-Cys and the precipitate was redispersed in 1 mL PBS. Then, 75 mM EDC and 15 mM NHS were added into the solution and reacted for 1 h to activate the carboxyl group. Since the C_3N_4 had plenitudinous $-NH_2$ group, the $C_{60}@C_3N_4$ nanocomposites could be easily synthetized by adding prepared

C_3N_4 with an incubation of 12 h. After centrifugation at 8000 rpm for 10 min, the $C_{60}@C_3N_4$ precipitate was redispersed in 1 mL PBS for further use.

2.2 Fabrication of PEC aptasensor

Prior to use, the bare GCEs were polished with 0.3 and 0.05 μm alumina slurry respectively, aiming to obtain a mirror-like surface for electrodeposition of an Au nanoparticle layer (depAu). Then, the cleaned GCEs were subjected to 2 mL $HAuCl_4$ solution (1 *wt*%) for 30 s electrodeposition at the potential of -0.2 V. After that, 5 μL prepared PTCA was thrown on the electrode for drying and then used PBS to undergo rinsing for getting rid of excess PTCA. After electrodeposition of another depAu on electrode with the deposition time of 15 s, 15 μL TBA I (2.0 mM) was dropped for 12 h to obtain a TBA I/depAu/PTCA/depAu/GCE platform via the strong binding ability between $-NH_2$ group of TBA I and depAu. To prevent the nonspecific adsorption on electrode, 15 μL HT (2.0 mM) was dropped on the resulting electrode and incubated for 40 min. Afterwards, the electrodes as a PEC biosensor was subjected to 20 μL thrombin with different concentrations for 40 min at 37 °C. Subsequently, the electrodes were immersed in 15 μL TBA II solution for 40 min to perform the typical sandwich-type reaction. Then, 10 μL glutaraldehyde was attached on electrode and reacted for 10 min, which subsequently followed by the incubation of 20 μL prepared $C_3N_4@C_{60}$ nanocomposites for 10 min. Finally, the modified electrodes were washed with PBS and dried before measurement. The design of $C_{60}@C_3N_4$ nanocomposites induced signal-off PEC aptasensor with depAu decorated PTCA as platform was shown in Scheme 1.

3. Results and discussion

3.1 Morphology and spectroscopic characterizations

The surface morphology of C_3N_4, C_{60} and $C_{60}@C_3N_4$ nanocomposites were investigated by the SEM. As illustrated in Fig. 1A and Fig. 1B, the C_3N_4 and C_{60} displayed a planar sheet-like and analogue circular morphology, respectively, which was consistent with the previous literatures[27], suggesting the successful synthesis of C_3N_4 and C_{60}. Studies have shown that the large surface area of C_3N_4, which structure derived from the graphite sheet, could provide abundant loading sites for other materials. Therefore, after the combination of C_3N_4 and C_{60} to form $C_{60}@C_3N_4$ nanocomposites, we observed that a large amount of C_{60} with small size was densely dispersed onto the surfaces of C_3N_4 nanosheet. And the Fig. 1C gave a readily visualizable morphology exhibition for that. Moreover, the UV–vis absorption spectroscopy was also used for measuring the as-prepared samples. The black line in Fig.1D was the spectrum of C_3N_4, which displayed no obviously absorption peak. However, the C_{60} functionalized with L-Cys showed two absorption peaks approximately at 260 and 360 nm, respectively (green line, Fig 1D), which was in line with other reported results[28]. Moreover, after the formation of $C_{60}@C_3N_4$ nanocomposites, the absorption showed a red-shift trend of the surface plasmon band (red line, Fig 1D), indicating the successful preparation of $C_{60}@C_3N_4$ nanocomposites.

3.2 PEC characterization of aptasensor.

The assembly process of aptasensor was investigated by photocurrent response. As displayed in Fig. 2, the bare GCE (curve a) and depAu/GCE (curve b) respectively showed negligible photocurrent signal owing to the absence of photoelectric material. After its modification on depAu/GCE, the photocurrent signal increased obviously since the PTCA possessed desirable photoelectric property (curve c). Then, the photocurrent intensity obviously enhanced after electrodeposition of another depAu layer (curve d). It was mainly because the depAu with SPR process could significantly improve light absorption and hinder recombination of electron/hole pairs. The photocurrent intensity successively decreased after the in turn assembly of TBAI and HT (curve e and f, respectively), which could be ascribed to the weak charge-transfer abilities of both DNA sequences and HT molecules. When the HT/TBAI/depAu/PTCA/depAu/GCE was subjected to 10 pM thrombin, the photocurrent intensity further decreased (curve g). It could be attributed to the inert property of protein. After modification of TBAII on electrode through a typical sandwich reaction, the photocurrent intensity also further decreased (curve h). Since the C_{60}@C_3N_4 nanocomposites could effectively hinder the electron translation, the photocurrent intensity decreased significantly when the modification of C_{60}@C_3N_4 nanocomposites (curve i). There are two reasons listed as follows: first, the C_3N_4 competed partly with PTCA in light absorption for producing a significantly smaller photocurrent in the presence of electron donor AA. Additionally, both the C_3N_4 and C_{60} have the poor conductivity, which could inhibit the electron transfer to achieve a further decreased photocurrent. Summarily, the expectably changed photocurrent

intensity suggested successful fabrication of the proposed aptasensor.

3.3 Comparison of various photoactive materials in the assistant of electron donor AA

To test the difference in photovoltaic conversion efficiency between C_3N_4 and PTCA, the PEC measurement in detection solution without and with electron donor AA by using C_3N_4/GCE and PTCA/GCE were performed, respectively. As shown in Fig. 3, the C_3N_4/GCE showed extremely low photocurrent change (Fig. 3A) compared with that of PTCA/GCE (Fig. 3B) after the addition of electron donor AA, suggesting that the electron donor AA could significantly improve the photovoltaic conversion efficiency of PTCA and much higher than that of C_3N_4, providing a possibility in constructing C_{60}@C_3N_4 nanocomposites induced "signal-off" PEC biosensor.

3.4 Comparison of different signal amplification strategies

To test the signal amplification of C_{60}@C_3N_4 nanocomposites, a comparison experiment with different electrodes was performed. Fig. 4 displayed the changes of photocurrent intensity after the HT/TBAI/depAu/PTCA/depAu/GCE incubating with 10 pM thrombin and further assembly of different probes. We can see that the photocurrent intensity of HT/TBAI/depAu/PTCA/depAu/GCE only changed 0.54 μA (Fig. 4A) after the incubation of thrombin, while the photocurrent intensity decreased about 1.84 μA after the further assembly of TBAII (Fig. 4B). Significantly, the photocurrent intensity changed the most about 4.04 μA after the decoration of C_{60}@C_3N_4 nanocomposites (Fig. 4C), suggesting the proposed method could effectively improve the sensitivity of aptasensor.

3.5 Analytical performance of PEC aptasensor for detection of thrombin.

The target thrombin with different concentrations was added respectively into the reaction system to monitor the analytical performance of proposed PEC aptasensor. As illustrated in Fig. 5A, the changes of photocurrent enlarged with the increase of thrombin concentrations from 10 fM to 10 nM, which was in accordance with the fact that thrombin with higher concentrations would induce more assembly of secondary DNA TBA II, thereby enabling more $C_{60}@C_3N_4$ nanocomposites bound with the TBAII to reduce the photocurrent intensity of PTCA. Moreover, the photocurrent changes showed linear relation to logarithm of thrombin concentrations. The equation of linear regression was $\Delta I = 0.6573\log c + 3.260$ ($r = 0.9967$, Fig. 5B). And the detection limit was 1.5 fM at the signal-tonoise ratio of 3. In addition, the sensitivity of the proposed PEC strategy was compared with that of some reported PEC assay as well as other analytical protocols. The corresponding results were shown in Table 1 and Table 2. We can see that the proposed biosensor offered a much better detection limit and a wider linear response scope, which suggested that the modification of $C_{60}@C_3N_4$ nanocomposites on secondary aptamer indeed could reduce the photocurrent intensity of PTCA significantly.

3.6 Selectivity, stability and reproducibility of the PEC aptasensor.

The selectivity of this assay was investigated by using hemoglobin (HB), bovine serum albumin (BSA), alpha fetoprotein (AFP), and L-Cys to substitute thrombin with the same concentration (10 pM), respectively. As shown in Fig. 6A, the presence

of thrombin could induce a remarkable photocurrent change, while HB, BSA, AFP and L-Cys had no obvious photocurrent change. Meanwhile, the obtained response from a mixture containing above four interferences and thrombin was almost the same as the response obtained from thrombin only. These results demonstrated that biosensing approach showed a high selectivity toward the target thrombin detection.

Additionally, we also evaluated the stability of this assay via consecutive cyclic light excitation. As indicated in Fig. 6B, there was no significant change of photocurrent density within 440 s under interrupted light excitation, which suggested an acceptable stability of the proposed PEC bioassay. Moreover, we further investigated the reproducibility of proposed aptasensor by using both intra-assay and inter-assay. The relative standard deviations (RSDs) of intra-assay were 4.65% and 3.23% at 0.1 and 100 pM, respectively. The inter-assay RSD of 5.32% and 3.58% were acquired by measuring the same thrombin samples of three electrodes prepared separately under the same conditions. These results suggested the superior reducibility of this PEC biosensor, thereby providing a stable sensing platform mainly due to the excellent membrane-forming property.

4. Conclusions

In summary, we here reported a novel C_{60}@C_3N_4 nanocomposites induced signal-off photoelectrochemical (PEC) aptasensor for sensitive detection of thrombin based on depAu decorated PTCA as sensing platform. The excellent membrane-forming of PTCA and SPR effect of depAu not only provided an extremely high initial photocurrent, but also made the assay system simple and sensitive. However, the C_3N_4 competed partly with PTCA in light absorption for

producing a significantly smaller photocurrent in the presence of electron donor AA after the introduce of C_{60}@C_3N_4 nanocomposites via typical sandwich reaction. At the same time, the C_3N_4 with high surface area can effectively improve the immobilization amount of inert C_{60} and partly competed with PTCA in light absorption for further improving the sensitivity of proposed biosensor. The method presented here was signal tag "label-free", low cost, simple in operation, and highly sensitive, which made it possible to detect thrombin for early diagnosis of various diseases.

Acknowledgement

This work was financially supported by the Chongqing Research Program of Basic Research and Frontier Technology (cstc2018jcyjA0797, cstc2017jcyjAX0230), the Fundamental Research Funds for the Central Universities (XDJK2019B022, SWU115037, XDJK2018C041), and the National Natural Science Foundation (NNSF) of China (21675129, 51473136).

References

1. S. Chen, P. Liu, K.W. Su, X. Li, Z. Qin, W. Xu, J. Chen, C.R. Li and J.F. Qiu, Electrochemical aptasensor for thrombin using co-catalysis of hemin/G-quadruplex DNAzyme and octahedral Cu_2O-Au nanocomposites for signal amplification, Biosens. Bioelectron. 99 (2018) 338-345.

2. Z.H. Su, X.L. Xu, H.T. Xu, Y. Zhang, C.R. Li, Y. Ma, D.C. Song and Q.J. Xie, Multi-DNAzymes-functionalized gold nanoparticles for ultrasensitive chemiluminescence detection of thrombin on microchip, Anal. Chim. Acta 1027

(2018) 76-82.

3. C.H. Zhu, W.Y. Zhu, L. Xu and X.M. Zhou, A label-free electrochemical aptasensor based on magnetic biocomposites with Pb^{2+}-dependent DNAzyme for the detection of thrombin, Anal. Chim. Acta 1047 (2019) 21-27.

4. A. Membrino, M. Paramasivam, S. Cogoi, J. Alzeer, N.W. Luedtke and L.E. Xodo, Cellular uptake and binding of guanidine-modified phthalocyanines to KRAS/HRAS G-quadruplexes, Chem. Commun. 46 (2010) 625-627.

5. L.J. Huang, L. Zhang, L. Yang, R. Yuan and Y.L. Yuan, Manganese porphyrin decorated on DNA networks as quencher and mimicking enzyme for construction of ultrasensitive photoelectrochemistry aptasensor, Biosens. Bioelectron. 104 (2018) 21-26.

6. H. Wang, F. Yuan, X.M. Wu, Y.M. Dong and G.L. Wang, Enzymatic in situ generation of covalently conjugated electron acceptor of PbSe quantum dots for high throughput and versatile photoelectrochemical bioanalysis, Anal. Chim. Acta 1058 (2019) 1-8.

7. N. Hao, Y. Zhang, H. Zhong, Z. Zhou, R. Hua, J. Qian, Q. Liu, H. Li and K. Wang, Design of a dual channel self-reference photoelectrochemical biosensor, Anal. Chem. 89 (2017) 10133-10136.

8. D. Wu, X. Xin, X. Pang, M. Pietraszkiewicz, R. Hozyst, X.G. Sun and Q. Wei, Application of europium multiwalled carbon nanotubes as novel luminophores in an electrochemiluminescent aptasensor for thrombin using multiple amplification strategies, Acs. Appl. Mater. Interfaces 7 (2015) 12663-12670.

9. X. Zhong, J.J. Lv, S. Xue, R. Yuan and Y.Q. Chai, An electrochemical assay based on acid-induced dissolution of nanoparticles to trigger enzyme-free cleavage for target detection, J. Electrochem. Soc. 165 (2018) B223-B226.

10. Y.Y. Liu, Y.H. Zhao, Q. Fan, M.S. Khan, X.J. Li, Y. Zhang, H.M. Ma and Q. Wei, Aptamer based electrochemiluminescent thrombin assay using carbon dots anchored onto silver-decorated polydopamine nanospheres, Microchim. Acta 185 (2018) 85-94.

11. J. Li, W.J. Zhou, R. Yuan and Y. Xiang, Aptamer proximity recognition-dependent strand translocation for enzyme-free and amplified fluorescent detection of thrombin via catalytic hairpin assembly, Anal. Chim. Acta 1038 (2018) 126-131.

12. J. Feng, C. Zhuo, X. Ma, S. Li and Y. Zhang, A peptide with a cysteine terminus: probe for label-free fluorescent detection of thrombin activity, Analyst 141 (2016) 4481-4487.

13. J.M. Wang, S.F. Mao, H.F. Li and J.M. Lin, Multi-DNAzymes-functionalized gold nanoparticles for ultrasensitive chemiluminescence detection of thrombin on microchip, Anal. Chim. Acta 1027 (2018) 76-82.

14. R. Hua, N. Hao, J. Lu, J. Qian, Q. Liu, H. Li and K. Wang, A sensitive potentiometric resolved ratiometric photoelectrochemical aptasensor for escherichia coli detection fabricated with non-metallic nanomaterials, Biosens. Bioelectron. 106 (2018) 57-63.

15. N. Hao, R. Hua, S. Chen, Y. Zhang, Z. Zhou, J. Qian, Q. Liu and K. Wang, Multiple signal-amplification via Ag and TiO_2 decorated 3D nitrogen doped

graphene hydrogel for fabricating sensitive label-free photoelectrochemical thrombin aptasensor, Biosens. Bioelectron. 101 (2018) 14-20.

16. A. Wicklein, A. Lang, M. Muth and M. Thelakkat, Swallow-tail substituted liquid crystalline perylene bisimides: synthesis and thermotropic properties, J. Am. Chem. Soc. 131 (2009) 14442-14453.

17. S. Gan, L. Zhong, L. Gao, D.X. Han and L. Niu, Electrochemically driven surface-confined acid/base reaction for an ultrafast H^+ supercapacitor, J. Am. Chem. Soc. 138 (2016) 1490-1493.

18. J. Han, Z. Wang, S. An, P. Dong, G. Xie and S. P. Chen, Facile synthesis of perylenetetracarboxylic acid modified bismuth@carbon nanostructures and its enhanced sensitivity for selective electrochemical determination of three biomolecules, J. Electrochem. Soc. 164 (2017) B553-B557.

19. J. Li, W.W. Tu, H.B. Li, M. Han, Y.Q. Lan, Z.H. Dai and J.C. Bao, In situ-generated nano-gold plasmon-enhanced photoelectrochemical aptasensing based on carboxylated perylene-functionalized graphene, Anal. Chem. 86 (2014) 1306-1312.

20. S.K. Cushing, J. Li, F. Meng, T.R. Senty, S. Suri, M.J. Zhi, M. Li, A.D. Bristow and N.Q. Wu, Photocatalytic activity enhanced by plasmonic resonant energy transfer from metal to semiconductor, J. Electrochem. Soc. 134 (2012) 15033-15041.

21. H. Da, H. Liu, Y.Y. Zheng, R. Yuan and Y.Q. Chai, A highly sensitive VEGF165 photoelectrochemical biosensor fabricated by assembly of aptamer bridged DNA

networks, Biosens. Bioelectron. 101 (2018) 213-218.

22. P.P. Li, X.P. Liu, C.J. Mao, B.K. Jin and J.J. Zhu, Photoelectrochemical DNA biosensor based on g-C_3N_4/MoS_2 2D/2D heterojunction electrode matrix and co-sensitization amplification with CdSe QDs for the sensitive detection of ssDNA, Anal. Chim. Acta 1048 (2019) 42-49.

23. H.Y. Wang, Q.J. Lu, M.X. Li, H. Li, Y.L. Liu, H.T. Li, Y.Y. Zhang and S.Z. Yao, Electrochemically prepared oxygen and sulfur co-doped graphitic carbon nitride quantum dots for fluorescence determination of copper and silver ions and biothiols, Anal. Chim. Acta 1027 (2018) 121-129.

24. H.M. Da, H.Y. Liu, Y.N. Zheng, R. Yuan and Y.Q. Chai, A highly sensitive VEGF165 photoelectrochemical biosensor fabricated by assembly of aptamer bridged DNA networks, Biosens. Bioelectron. 101 (2018) 213-218.

25. H.M. Deng, L.J. Huang, Y.Q. Chai, R Yuan and Y.L. Yuan, Ultrasensitive photoelectrochemical detection of multiple metal ions based on wavelength-resolved dual-signal output triggered by click reaction, Anal. Chem. 91 (2019) 2861-2868.

26. Z.K. Wang, X. Gong, M. Li, Y. Hu, J.M. Wang, H. Ma and L.S. Liao, Induced crystallization of perovskites by a perylene underlayer for high-performance solar cells, Acs. Nano 10 (2016) 5479-5489.

27. H. Yu, L. Shang, T. Bian, R. Shi, G. Waterhouse, Y.F. Zhao, C. Zhou, L.Z. Wu, C.H. Tung and T.R. Zhang, Nitrogen-doped porous carbon nanosheets templated from g-C_3N_4 as metal-free electrocatalysts for efficient oxygen reduction reaction,

Adv. Mater. 28 (2016) 5140-5140.

28. X. Zhong, R. Yuan and Y.Q. Chai, In situ spontaneous reduction synthesis of spherical Pd@Cys-C_{60} nanoparticles and its application in nonenzymatic glucose biosensors, Chem. Commun. 48 (2011) 597-599.

29. Y. Hou, J. Liu, M. Hong, X. Li, Y. Ma, Q. Yue and C. Li, A reusable aptasensor of thrombin based on DNA machine employing resonance light scattering technique, Biosens. Bioelectron. 92 (2017) 259-265.

30. S.B. Xie, J. Ye, Y.L. Yuan, Y.Q. Chai and R. Yuan, A multifunctional hemin@metal–organic framework and its application to construct an electrochemical aptasensor for thrombin detection, Nanoscale 7 (2015) 18232-18238.

31. H. Xu, S. Liang, X. Zhu, X. Wu, Y. Dong, H. Wu, W. Zhang and Y. Chi, Enhanced electrogenerated chemiluminescence behavior of C_3N_4 QDs@ C_3N_4 nanosheet and its signal-on aptasensing for platelet derived growth factor, Biosens. Bioelectron. 92 (2016) 695-701.

32. H. Cho, B.R. Baker, S. Wachsmannhogiu, C.V. Pagba, T.A. Laurence, S.M. Lane, L.P. Lee and J.B. Tok, Aptamer-based SERRS sensor for thrombin detection, Nano Letters 8 (2018) 4386-4390.

33. Y. Cao, Z.H. Wang, J.P. Cao, X.X. Mao, G.F. Chen and J. Zhao, A general protein aptasensing strategy based on untemplated nucleic acid elongation and the use of fluorescent copper nanoparticles: Application to the detection of thrombin and the vascular endothelial growth factor, Microchim. Acta 184 (2017) 3697-3704.

34. L. Wang, W. Yang, T.F. Li, D, Li, Z.M. Cui, Y. Wang, S.L. Ji, Q.X. Song, C. Shu and L. Ding, Colorimetric determination of thrombin by exploiting a triple enzyme-mimetic activity and dual-aptamer strategy, Microchim. Acta 184 (2017) 3145-3151.

35. C. Du, Y. Hu, Q. Zhang, Z. Guo, G. Ge, S. Wang, C. Zhai and M. Zhu, Competition-derived FRET-switching cationic conjugated polymer-Ir(III) complex probe for thrombin detection, Biosens. Bioelectron. 100 (2017) 132-138.

36. Y. Bai, F. Feng, L. Zhao, C. Wang, H. Wang, M. Tian, J. Qin, Y. Duan and X. He, Aptamer/thrombin/aptamer-AuNPs sandwich enhanced surface plasmon resonance sensor for the detection of subnanomolar thrombin, Biosens. Bioelectron. 47 (2013) 265-270.

37. Y.W, G.A. Le, N. Spinelli, M. Holzinger, G.W. Diao, D. Shan, E. Defrancq and S. Cosnier, Electrogenerated trisbipyridyl Ru(II)-/nitrilotriacetic-polypyrene copolymer for the easy fabrication of label-free photoelectrochemical immunosensor and aptasensor: Application to the determination of thrombin and anti-cholera toxinantibody, Biosens. Bioelectron., 42 (2013) 556-562.

38. X. Zhang, Y. Xu, Y. Yang, X. Jin, S. Ye, S. Zhang and L. Jiang, A new signal-on photoelectrochemical biosensor based on a graphene/quantum-dot nanocomposite amplified by the dual−quenched effect of bipyridinium relay and AuNPs, Chemistry 18 (2012) 16411-16418.

39. Y. Liu, K. Yan, O.K. Okoth and J. Zhang, A label-free photoelectrochemical aptasensor based on nitrogen-doped graphene quantum dots for chloramphenicol

determination, Biosens. Bioelectron. 74 (2015) 1016-1021.

40. K. Yan, Y. Liu, Y. Yang and J. Zhang, A cathodic “signal-off” photoelectrochemical aptasensor for ultrasensitive and selective detection of oxytetracycline, Anal. Chem. 87 (2015) 12215-12220.

41. S. Li, W. Zhu, Y. Xue and S. Liu, Construction of photoelectrochemical thrombin aptasensor via assembling multilayer of graphene–CdS nanocomposites, Biosens. Bioelectron. 64 (2015) 611-617.

42. X. Zhang, S. Li, X. Jin and S. Zhang, A new photoelectrochemical aptasensor for the detection of thrombin based on functionalized graphene and CdSe nanoparticles multilayers, Chem. Commun. 47 (2011) 4929-4931.

Scheme 1 Schematic illustration of (A) the preparation of $C_{60}@C_3N_4$ nanocomposites and (B) $C_{60}@C_3N_4$ nanocomposites induced signal-off PEC aptasensor with depAu decorated PTCA as platform.

Fig. 1 The SEM images of (A) C_3N_4, (B) C_{60} and (C) $C_{60}@C_3N_4$ nanocomposites. (D) The UV spectrum of C_3N_4 (black line), C_{60} (green line) and $C_{60}@C_3N_4$ nanocomposites (red line).

Fig. 2 Photocurrent responses of (a) GCE, (b) depAu/GCE, (c) PTCA/depAu/GCE, (d) depAu/PTCA/depAu/GCE, (e) TBAI/depAu/PTCA/depAu/GCE, (f) HT/TBAI/ depAu/PTCA/depAu/GCE, (g) thrombin/HT/TBAI/depAu/PTCA/depAu/GCE, (h) TBAII/thrombin/HT/TBAI/depAu/PTCA/depAu/GCE and (i) TBAII/thrombin/HT/ TBAI/depAu/PTCA/depAu/GCE after the immobilization of $C_{60}@C_3N_4$ nanocomposites.

Fig. 3 Photocurrent responses of (A) C_3N_4/GCE and (B) PTCA/GCE investigated in PBS buffer without and with electron donor AA.

Fig. 4 The comparison experiment of photocurrent change for the HT/TBAI/depAu /PTCA/depAu/GCE incubating with 10 pM thrombin (A), and further assembly of TBAII (B) and $C_{60}@C_3N_4$ nanocomposites (C).

Fig. 5 (A) Photocurrent responses of the PEC aptasensor for different thrombin concentrations: 10 fM, 100 fM, 1 pM, 10 pM, 100 pM, 1 nM and 10 nM. (B) The corresponding calibration curve (n =3). The PEC measurements were performed in 0.1 M PBS containing 2 mM electron donor AA with the excitation light source at 365 nm by the LED lamp and switched off-on-off for 10-20-10 s under 0.0 V potential.

Fig. 6 (A) Specificity of the biosensor. (B) The PEC stability of proposed aptasensor with 10 nM thrombin under periodic off-on-off light for 11 cycles.

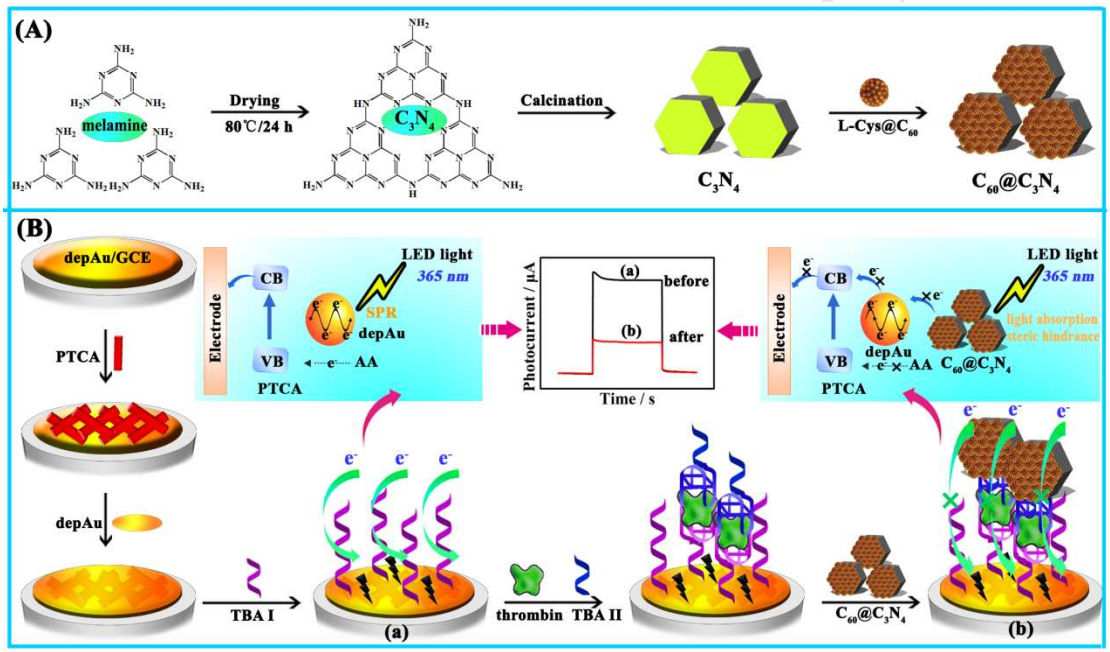
(A)
melamine
Drying
80℃/24 h
C_3N_4
Calcination
C_3N_4
L-Cys@C_{60}
$C_{60}@C_3N_4$
(B)
depAu/GCE
PTCA
depAu
TBA I
(a)
Electrode
CB
VB
PTCA
LED light
365 nm
SPR
depAu
AA
Photocurrent / μA
Time / s
(a)
before
(b)
after
thrombin
TBA II
$C_{60}@C_3N_4$
light absorption
steric hindrance
(b)

Scheme 1

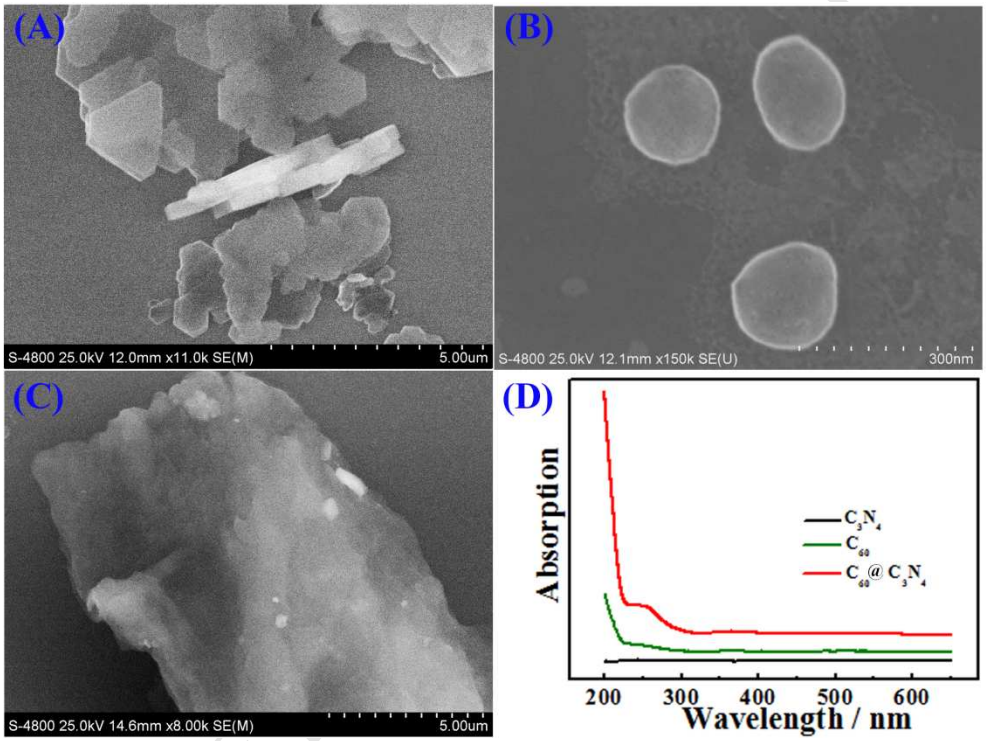
(A)
S-4800 25.0kV 12.0mm x11.0k SE(M)
5.00um
(B)
S-4800 25.0kV 12.1mm x150k SE(U)
300nm
(C)
S-4800 25.0kV 14.6mm x8.00k SE(M)
5.00um
(D)
Absorption
C3N4
C60
C60@C3N4
200
300
400
500
600
Wavelength / nm

Fig. 1

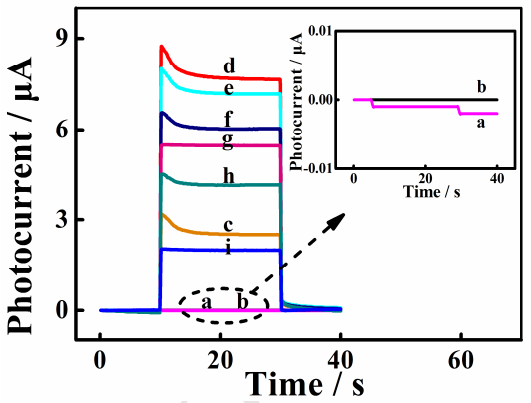

Fig. 2

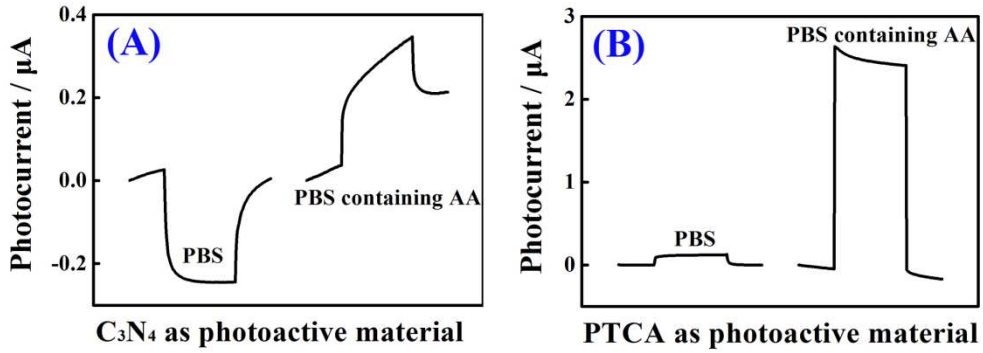

Fig. 3

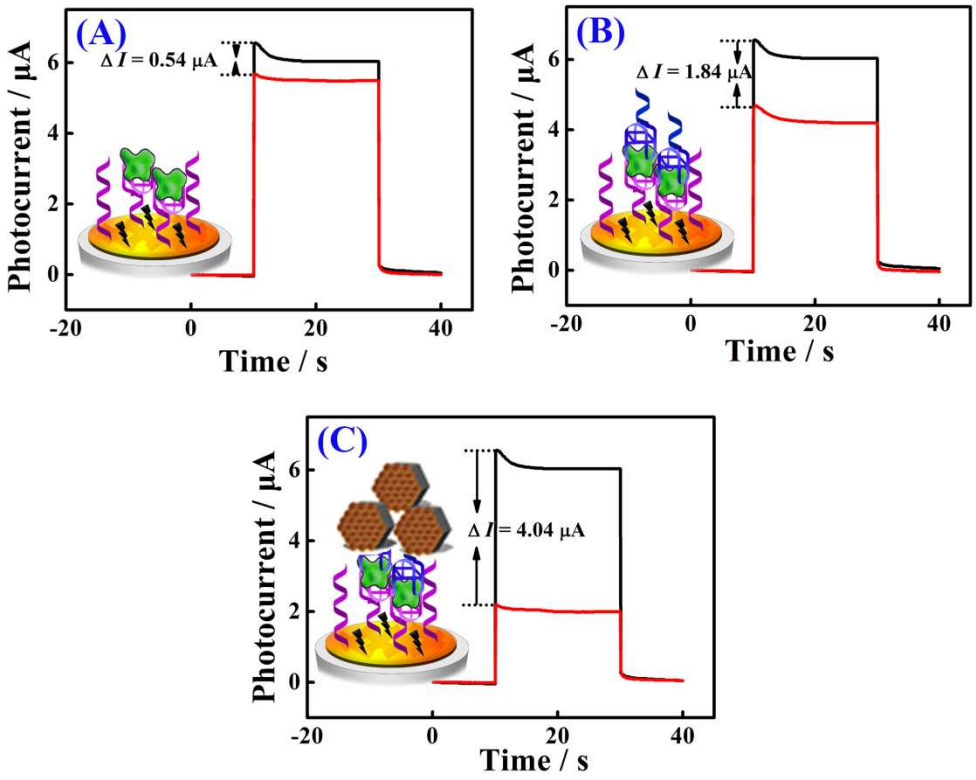

Fig. 4

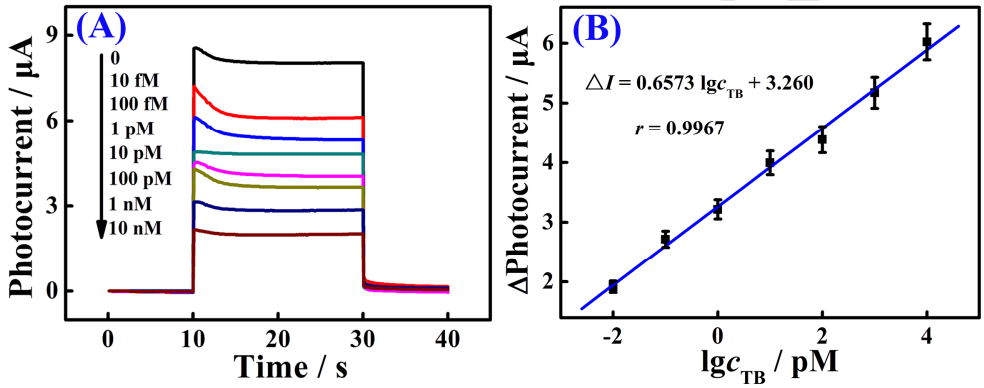
(A)
0
10 fM
100 fM
1 pM
10 pM
100 pM
1 nM
10 nM
Photocurrent / μA
Time / s
(B)
△I = 0.6573 lgc_TB + 3.260
r = 0.9967
ΔPhotocurrent / μA
lgc_TB / pM

Fig. 5

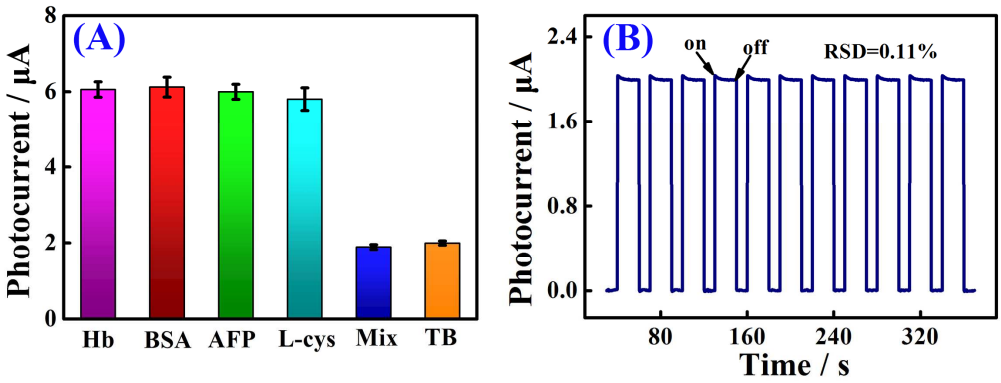

Fig. 6

Table 1 Comparisons of the proposed PEC biosensor with different methods for thrombin detection.

Analytical method	Linear range	Detection limit	Ref.
RLS	60 pM-6 nM	3.5 pM	29
EC	0.0001-30 nM	0.068 pM	30
ECL	0.5-40 nM	0.08 nM	31
SERRS	100 pM-1 μM	100 pM	32
FL	0.01-0.12 nM	0.04 nM	33
EIS	0.12-30 nM	0.06 pM	34
FRET	0.05- 200 pM	0.05 pM	35
SPR	0.1 -75 nM	0.1 nM	36
PEC	10 fM-10 nM	1.5 fM	Our work

Abbreviation: resonance light scattering (RLS); electrochemistry (EC); fluorescence (FL); electrochemiluminescence (ECL); surface-enhanced resonant Raman scattering (SERRS); electrochemical impedance spectroscopy (EIS); resonance energy transfer (FRET); surface plasmon resonance (SPR).

Table 2 Comparisons of proposed biosensor with other reported PEC biosensors for TB detection.

Analytical method	Linear range	Detection limit	Ref.
PEC	0-10 pM	0.1 pM	37
PEC	20-200 fM	5.9 fM	38
PEC	10-250nM	3.1 nM	39
PEC	4.0-150nM	0.9 nM	40
PEC	2.0-600 pM	1.0 pM	41
PEC	1.0-10pM	0.45 pM	42
PEC	10 fM-10nM	1.5 fM	Our work

Highlights

- A signal-off photoelectrochemical (PEC) aptasensor was proposed for sensitive detection of thrombin on the basis of C_{60}@C_3N_4 nanocomposites as quencher and Au nanoparticles (depAu) decorated perylene tetracarboxylic acid (PTCA) as sensing platform.
- The PTCA between two depAu layers can simply and effectively produce an extremely high initial photocurrent to afford a precondition for sensitive biodetection.
- The C_3N_4 with high surface area not only provided massive binding sites for C_{60} immobilization, but also partly competed with PTCA in light absorption for producing a significantly smaller photocurrent in the presence of electron donor ascorbic acid (AA).
- Both the C_3N_4 and C_{60} with poor conductivity could inhibit the electron transfer to achieve a further decreased photocurrent for sensitivity improvement.

Declaration of interests

☐ The authors declare that they have no known competing financial interests or personal relationships that could have appeared to influence the work reported in this paper.

Yali Yuan

The authors declare no conflict of interest.